Available on CMS information server

**CMS NOTE 2010/008**

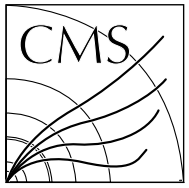


**The Compact Muon Solenoid Experiment**

**CMS Note**

Mailing address: CMS CERN, CH-1211 GENEVA 23, Switzerland

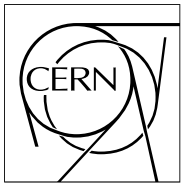


**5th May 2010**

# The CMS physics reach for searches at 7 TeV

The CMS Collaboration

**Abstract**

Some examples of the expected reach of CMS in terms of searches for new physics, for a proton-proton centre-of-mass energy of 7 TeV, are shown. Integrated luminosities between 100 $pb^{-1}$ and 1 $fb^{-1}$ are considered. The prospects are preliminary, and based on existing studies at higher energies.

# 1 Introduction

The LHC has recently started delivering proton-proton collisions at a centre-of-mass energy of 7 TeV. It is foreseen to run at this energy through autumn 2011, with a target integrated luminosity of 1 fb$^{-1}$. The physics reach of CMS has been described in detail in Ref. [1], assuming the LHC design centre-of-mass energy (14 TeV). Several studies have been also made at 10 TeV, as shown during the 2009 Summer Conferences [2].

Some examples of the expected physics reach of CMS, at a proton-proton centre-of-mass energy of 7 TeV, are described in this short note. Integrated luminosities between 100 pb$^{-1}$ and 1 fb$^{-1}$ are considered. The estimates are generally based on extrapolations from existing studies at higher energies, by applying simple scaling of cross sections for signal and backgrounds. No attempts of analysis reoptimization at 7 TeV have been made. As such, the results given in this note should be considered as a rough indication of the new physics reach of CMS at 7 TeV, pending more detailed studies.

In the next Section, a few examples of the expected CMS physics performance at 7 TeV, for various Beyond-the-Standard-Model scenarios (called Exotica in this note), are shown. In Section 3 it is shown that, at a centre-of-mass energy of 7 TeV, two representative analyses can significantly extend the experimental investigation of the Minimal Supersymmetric Standard Model (MSSM). Finally in the last section, the main plots related to the search for the Standard Model Higgs boson are updated at 7 TeV. One example of an alternative scenario (neutral Higgs boson in the MSSM) is also shown.

# 2 Scaling of Selected Exotica Results

In this section we discuss the scaling to 7 TeV of several recent Exotica results, originally obtained for 10 TeV or 14 TeV LHC running scenarios [3, 4, 5, 6, 7, 8, 9, 10, 11, 12]. In most of the cases, this scaling has been done using parton luminosity ratios for $q\bar{q}$ and $gg$ interactions as a function of the invariant mass of the system [13]. These ratios were obtained using MSTW2008NLO parton distribution functions [14] and are shown in Fig. 1.

As already mentioned, none of the results presented here were obtained via full analysis with proper reoptimization of the cuts, so they should be considered as conservative rough estimates of the true reach at 7 TeV. Nevertheless, the scaling results give a pretty consistent picture that running the machine at 7 TeV requires approximately three times higher integrated luminosity compared to that in a 10 TeV run in order to reach the same sensitivity.

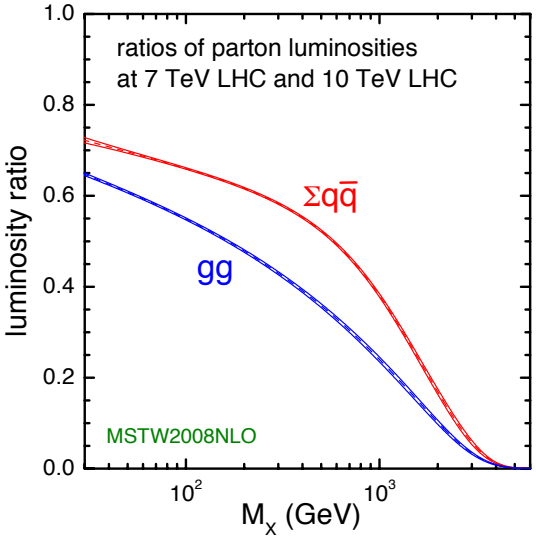


Figure 1: Ratio of parton luminosities for the LHC operating at 7 TeV and 10 TeV, as a function of the invariant mass of the produced final state. Courtesy James Stirling.

For the $b' \to tW$ analysis the parton luminosity ratio was not used; instead we used LO PYTHIA [15] cross sections for the signal and backgrounds at 7 TeV. The sensitivity of the search is shown in Fig. 2 for integrated luminosities of 200 and 600 pb$^{-1}$. Compared to the results of Ref. [3], approximately 3.5 times more integrated luminosity is required for a 7 TeV LHC run to match the reach at 10 TeV. With $\sim$ 100 pb$^{-1}$ of 7 TeV data, our sensitivity is expected to surpass the current Tevatron lower $b'$ mass limit of 325 GeV (95% C.L.) [16].

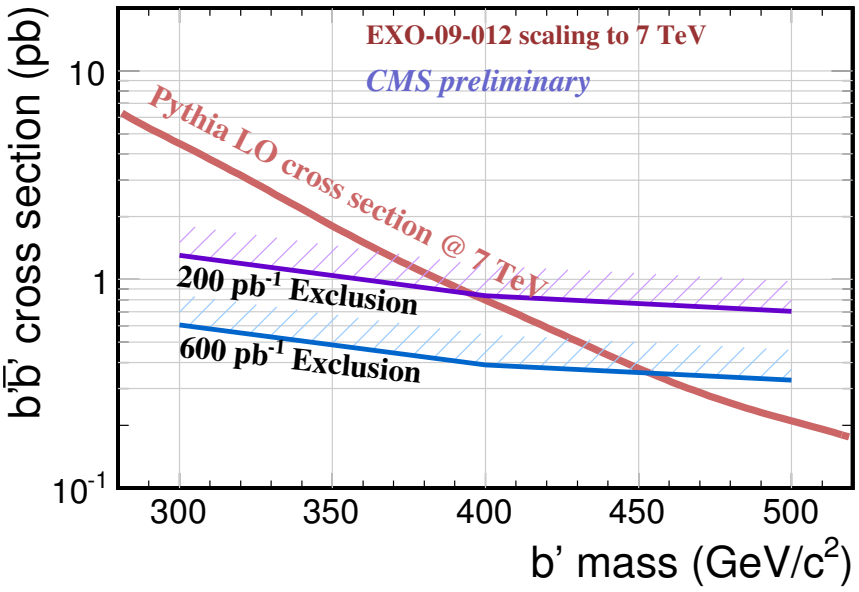


Figure 2: 95% C.L. limits on the $b'$ mass for a 7 TeV LHC run with an integrated luminosity of 200 and 600 pb$^{-1}$.

| $n_{ED}$ | 95% C.L. Lower Limits on $M_S$ | | |
|---|---|---|---|
| | 50 pb$^{-1}$ | 100 pb$^{-1}$ | 200 pb$^{-1}$ |
| 2 | 2.0 TeV | 2.2 TeV | 2.4 TeV |
| 3 | 2.5 TeV | 2.7 TeV | 2.9 TeV |
| 4 | 2.1 TeV | 2.2 TeV | 2.4 TeV |
| 5 | 1.9 TeV | 2.0 TeV | 2.2 TeV |
| 6 | 1.7 TeV | 1.9 TeV | 2.0 TeV |
| 7 | 1.6 TeV | 1.8 TeV | 1.9 TeV |

Table 1: Diphoton search for large extra-dimensions. Table of 95% C.L. limits on the ultraviolet cutoff scale ($M_S$) as a function of the number of extra dimensions $n$ for three characteristic integrated luminosities expected to be reached in a 7 TeV LHC run.

The two diphoton searches for large extra dimensions [4] and Randall-Sundrum (RS) gravitons [5] used the $q\bar{q}$ parton luminosity ratio at the diphoton system invariant mass of 500 GeV (the minimum mass requirement used in the analyses) in order to scale the dominant direct diphoton QCD background (which falls exponentially above this cutoff). For the RS graviton signal we used the $gg$ scaling factor evaluated at the graviton mass. Signal scaling for models with large extra dimensions is more complicated, as the signal is broad and also peaks at different mass values for different numbers of extra dimensions and different values of the model parameter $M_S$. Consequently, for each signal point a separate scaling, based on the $gg$ parton luminosity ratio at the average invariant mass of the signal, was used. The resulting 95% C.L. limits on the ultraviolet cutoff scale, $M_S$, in the model with large extra dimensions for different numbers of extra dimensions ($n$) are shown in Table 1, while the luminosity needed to reach an evidence (discovery) significance of 3 (5) standard deviations is shown in Fig. 3. The 95% C.L. limits and the discovery reach for RS gravitons are shown in Fig. 4. One can see that in models with large extra dimensions significantly higher (a factor of $\approx 8$) luminosity is required in a 7 TeV run compared to that at 10 TeV. Nevertheless, even with 50 pb$^{-1}$ of 7 TeV data, the sensitivity of the search already surpasses the current Tevatron limits [17]. For the RS case, the equivalent luminosity for a 7 TeV run is $\approx 4$ times higher than that at 10 TeV. Again, with just 50 pb$^{-1}$ of 7 TeV data the sensitivity of the search surpasses that at the Tevatron [18, 19].

For the search for large extra dimensions in the monojet channel [6], we used parton luminosity scaling for the signal and LO PYTHIA cross sections for backgrounds. Similar to the diphoton case, we scaled the signal at its mean value in terms of $\sqrt{\hat{s}}$. Since the signal is dominated by the $gg$ and $qg$ processes, which contribute approximately equally to graviton production, at the characteristic values of $M_D$ we are able to probe with early data, an average between the $gg$ and $qg$ parton luminosity scaling was taken for the signal scaling. As the $qg$ contribution has not been evaluated in Fig. 1, the geometric mean of the $gg$ and $q\bar{q}$ contributions was used for the estimate. The 95% C.L. exclusion limit and the discovery potential are shown in Fig. 5. Approximately 3 times the

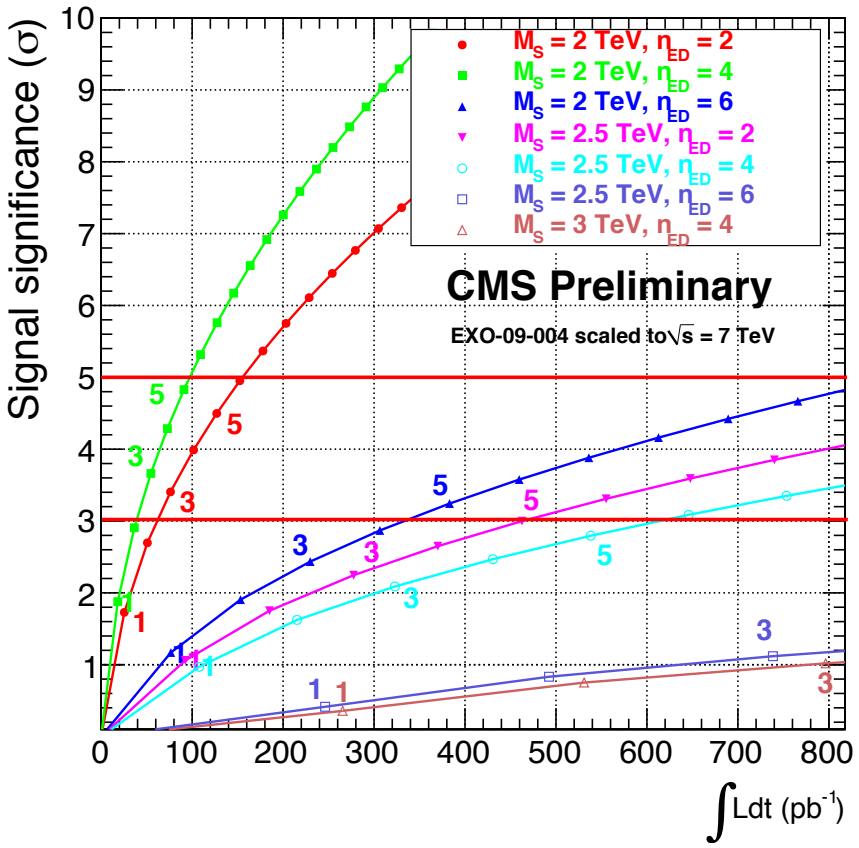


Figure 3: Discovery potential for large extra dimensions in the diphoton channel as a function of integrated luminosity of the LHC running at 7 TeV. The numbers on the curve correspond to the expected observed signal events.

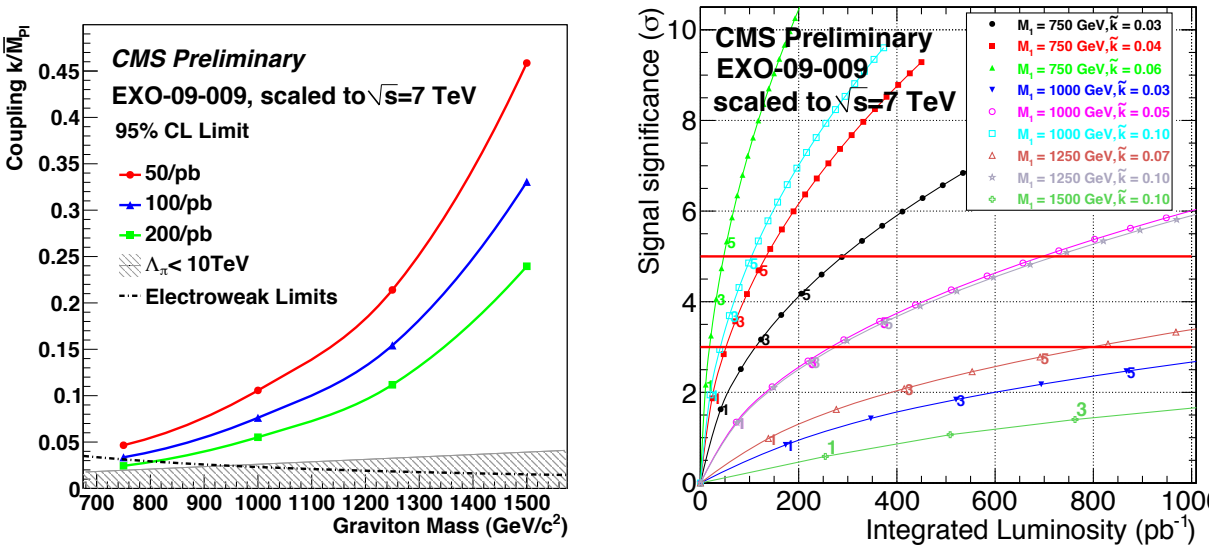


Figure 4: The 95% C.L. limit (left) and the discovery potential (right) for Randall-Sundrum gravitons in the diphoton channel, as a function of integrated luminosity at the LHC running at 7 TeV.

integrated luminosity of a 10 TeV run is required to reach similar sensitivity at 7 TeV. Even with as little as 10 pb$^{-1}$ of integrated luminosity the sensitivity of the search is expected to surpass that at the Tevatron [20], provided that missing transverse energy tails are understood well in early LHC data.

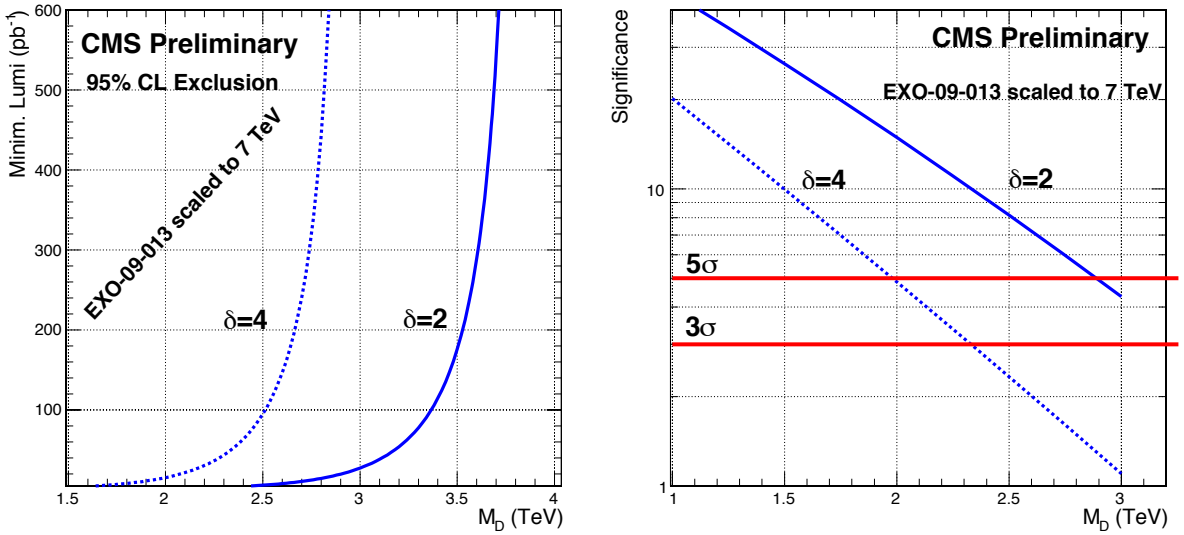


Figure 5: The 95% C.L. limit (left) as a function of integrated luminosity and the discovery potential (right) for an integrated luminosity of 200 pb$^{-1}$, for large extra dimensions in the monojet channel at the LHC running at 7 TeV.

For the first [7] and second [8] generation leptoquark searches we used $gg$ parton-luminosity scaling at twice the LQ mass for the signal, while $gg$ (top) and $q\bar{q}$ ($Z$+jets) scaling, at $\sqrt{\hat{s}}$ equal to the $S_T$ cut, was used for the exponentially falling background. The limits and discovery reach for 100 pb$^{-1}$ of the LHC data at 7 TeV are shown in Figs. 6, 7. Approximately three times higher integrated luminosity is needed to reach the same sensitivity as at 10 TeV. Even with $\sim$ 10 pb$^{-1}$ the LHC sensitivity at 7 TeV is expected to surpass that at the Tevatron [21] for both leptoquark generations.

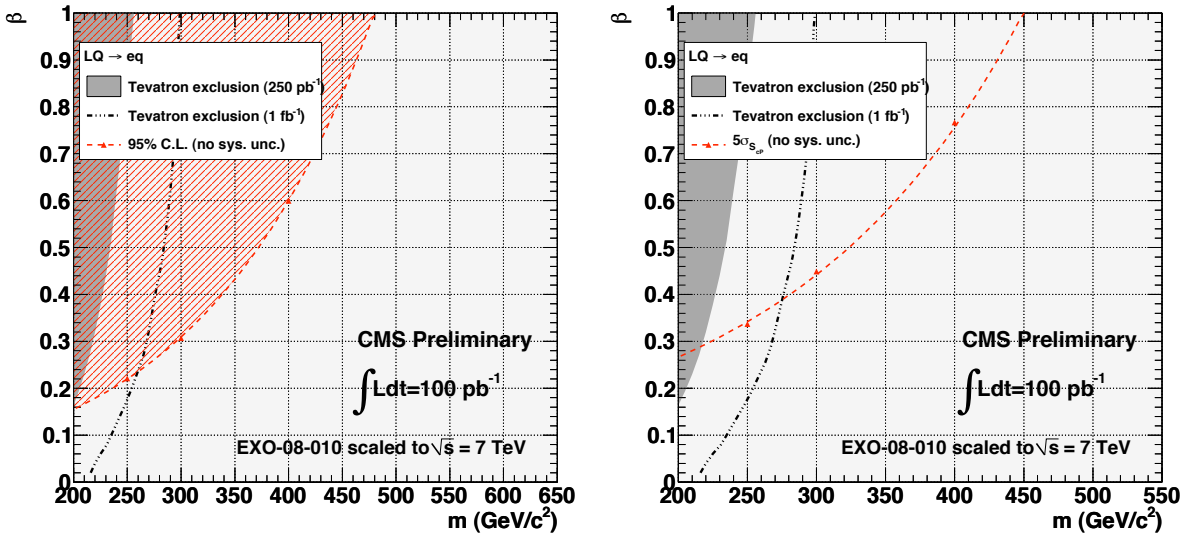


Figure 6: The 95% C.L. limit (left) and the discovery potential (right) for first generation leptoquarks as a function of their branching fraction ($\beta$) into a charged lepton for 100 pb$^{-1}$ of data at 7 TeV.

For the scaling of the $Z'$ and RS Kaluza-Klein gravitons in the dielectron [9] and dimuon [10] channels, we used the cross section from LO PYTHIA at 7 TeV; for the backgrounds, dominated by Drell-Yan, the cross section was

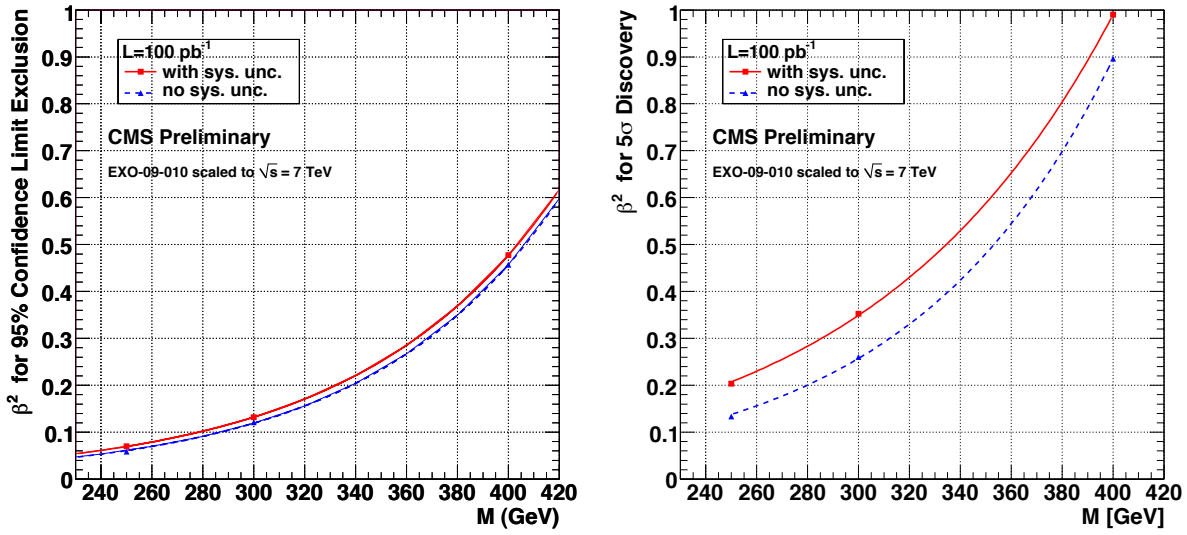


Figure 7: The 95% C.L. limit (left) and the discovery potential (right) for second generation leptoquarks as a function of their branching fraction ($\beta$) into a charged lepton for 100 pb$^{-1}$ of data at 7 TeV.

also taken from the LO generator. The limits and discovery reach are shown in Fig. 8 for the dielectron and in Fig. 9 for the dimuon channel. Approximately three (ten) times the luminosity of a 10 (14) TeV run is needed to reach similar sensitivity in a 7 TeV run. The sensitivity of the Tevatron searches [19, 22] will be superseded with approximately 100 pb$^{-1}$ of 7 TeV data.

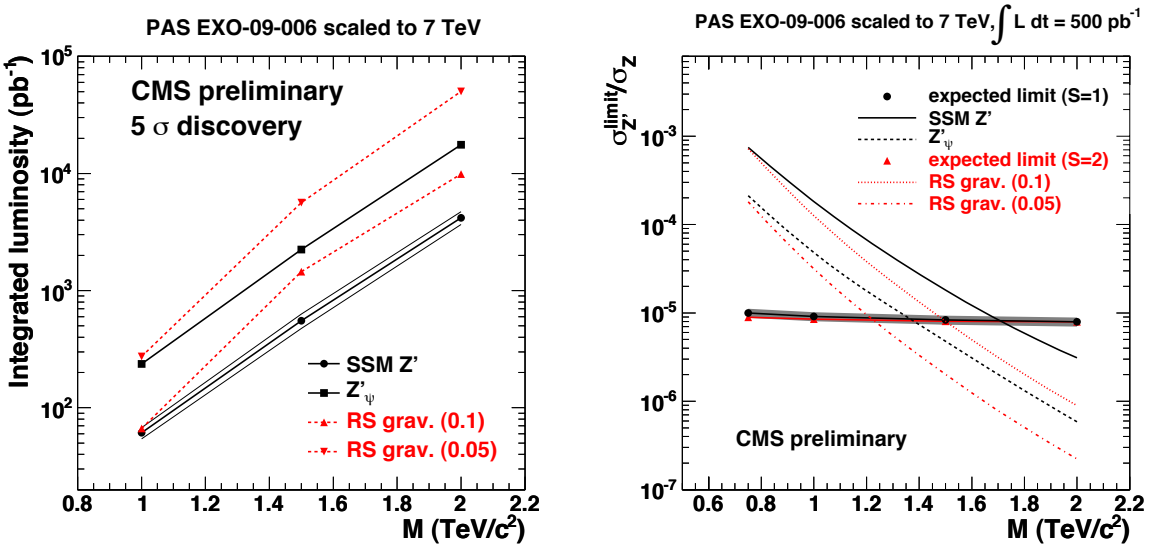


Figure 8: Discovery potential at 5$\sigma$ significance (left) and the 95% C.L. limit (right) for the $Z'$ and Randall-Sundrum gravitons in the $ee$ channel at 7 TeV.

The scaling of the search for Heavy Stable Charged Particles (HSCP) [11] was done using LO PYTHIA cross sections at 7 TeV for the signals. Since the background for this search is negligible, only the signal cross section matters. The 95% C.L. limits on gluinos and top squarks, as well as the discovery potential based on the observation of 3 data events, are shown in Fig. 10 as a function of the integrated luminosity. The discovery potential for the stau is also shown. The reach beyond the Tevatron limits [23] is achieved in the gluino and stop searches with just a few pb$^{-1}$ of 7 TeV data. Approximately ten times more data are needed to reach the same sensitivity in a 7 TeV run as in a 14 TeV run.

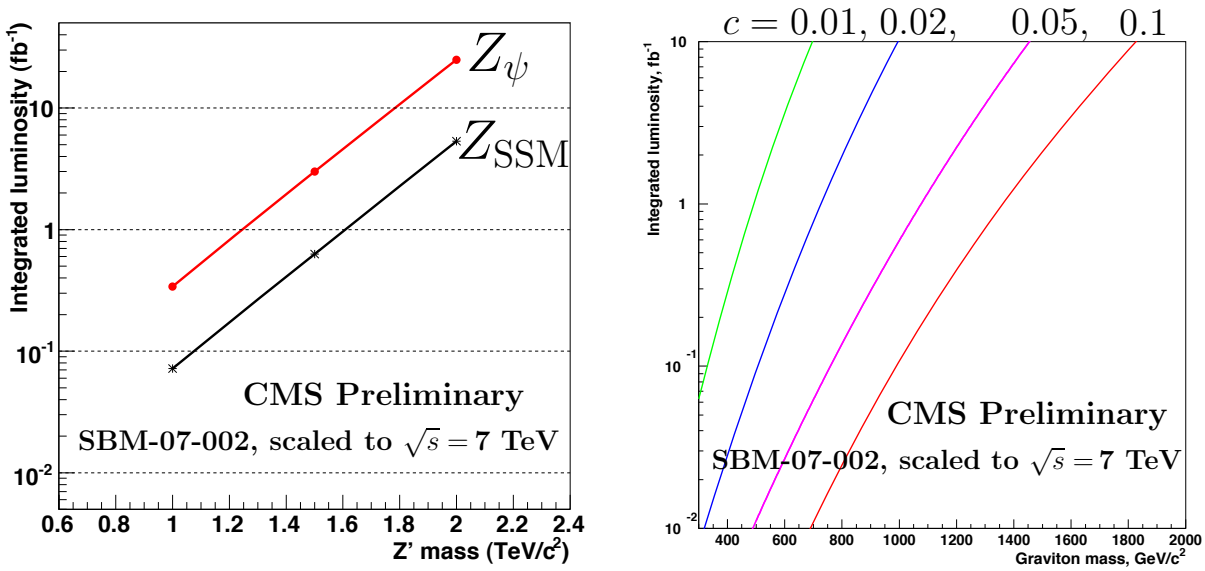


Figure 9: Discovery potential at $5\sigma$ significance for the $Z'$ (left) and Randall-Sundrum gravitons (right) in the $\mu\mu$ channel at 7 TeV.

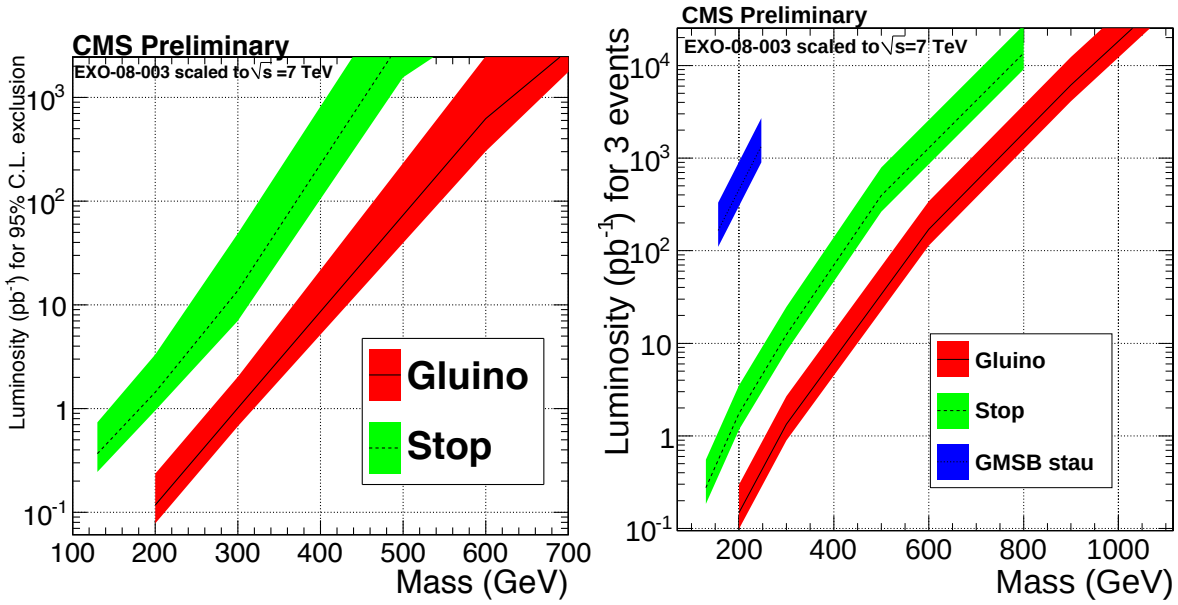


Figure 10: The 95% C.L. limit (left) and the discovery potential (right) for HSCP searches at 7 TeV. A tracker-only analysis is used to set 95% C.L. limits. For the discovery plot a combination of tracker and timing info in the CMS muon system's drift tubes is used; an integrated luminosity corresponding to 3 events is considered, since backgrounds for this search are negligible.

The scaling of the search for stopped gluinos [12] was done using the $gg$ parton luminosity scaling for the signal at $\sqrt{\hat{s}}$ of twice the gluino mass. Since the search is done during periods of no beam activity in the detector, the background does not depend on the machine energy and stays the same as in the 10 TeV analysis. The reach for stopped gluinos with a mass of 300 GeV with various lifetimes for instantaneous luminosities of $10^{32}$ cm$^{-2}$s$^{-1}$ and $10^{31}$ cm$^{-2}$s$^{-1}$ is shown in Fig. 11. While the discovery beyond the Tevatron limits [24] is possible with just a couple of weeks of data at high luminosity, it is remarkable that at low luminosity one can't even see an evidence for these particles, no matter how long the running period is. This is quite different from the 10 TeV situation [12] and is a solid physics case to push for higher instantaneous luminosity in the 2010 run. Finally, the reach for stopped gluinos as a function of their mass for the $10^{32}$ cm$^{-2}$s$^{-1}$ case is shown in Fig. 12.

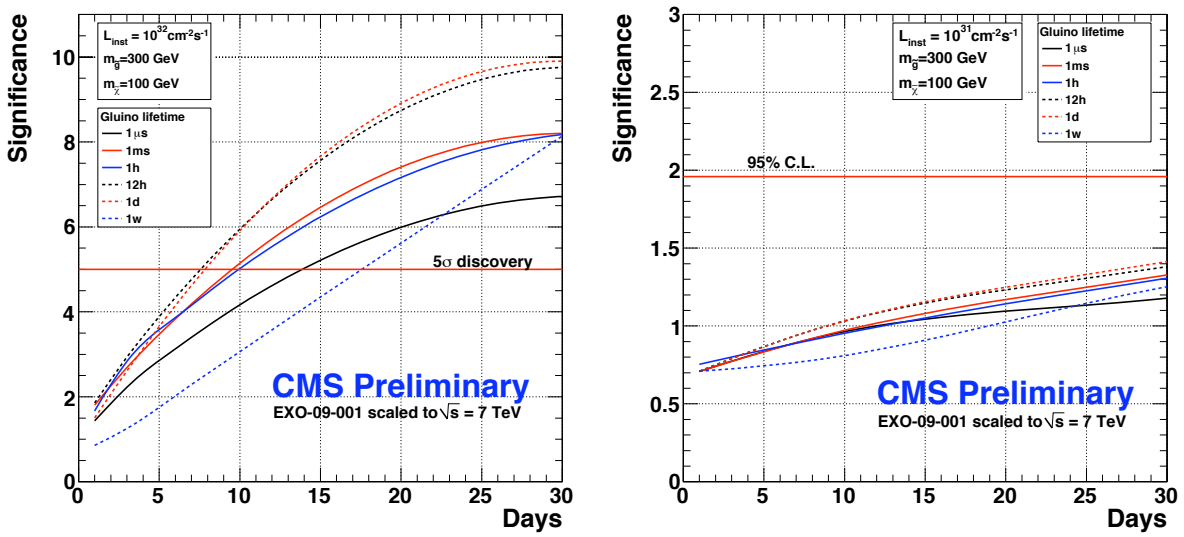


Figure 11: The discovery potential for a long-lived 300 GeV heavy gluino stopping in the CMS calorimeter in a 7 TeV run at an instantaneous luminosity of $10^{32}$ cm$^{-2}$s$^{-1}$ (left) and $10^{31}$ cm$^{-2}$s$^{-1}$ (right), as a function of the data-taking duration.

All in all, our scaling exercise demonstrates that the discovery of certain Exotica particles is still possible with $\sim 100$ pb$^{-1}$ of 7 TeV data. For most of the channels studied, running the machine at lower energy requires about 3 (10) times more data to exceed current sensitivity compared to that in a 10 (14) TeV run. The two exceptions are the searches for large extra dimensions via virtual graviton exchange [4], where approximately 8 times the luminosity is needed at 7 TeV, and the search for stopped gluinos [12], where an instantaneous luminosity of $\sim 10^{32}$ cm$^{-2}$s$^{-1}$ is essential to go beyond the Tevatron limits.

# 3 Sensitivity of CMS Supersymmetry Searches at $\sqrt{s} = 7$ TeV

CMS will perform a broad range of searches for supersymmetric (SUSY) particles [25]. The initial searches will be performed in a variety of inclusive final states involving jets, leptons, photons, and missing tranverse momentum ($p_T^{\rm miss}$). Backgrounds will be determined using data-driven methods whenever possible, with multiple methods for crosschecks. We focus here on the estimated sensitivities of searches in two key final states: the all-hadronic channel and the like-sign dilepton channel. The all-hadronic channel, in which the signature is based on the presence of high $p_T$ jets and large missing momentum $p_T^{\rm miss}$, has a relatively high efficiency for many SUSY models, but it also has substantial backgrounds from a large number of standard model processes. The like sign-dilepton channel, in contrast, is very powerful in suppressing standard model backgrounds, but the expected number of signal events is typically much smaller than in the hadronic final state.

Limitations on sensitivity estimates stem from two main issues: first, the lack of a preferred SUSY model or even a set of preferred SUSY models, and second, our current lack of complete knowledge on the size of backgrounds and the size of the (eventual) experimental systematic uncertainties on those backgrounds.

Theorists have long noted that the models commonly adopted for use as benchmarks, such as mSUGRA, do not span the full range of reasonable phenomenlogical patterns for which experimenters should search [26, 27, 28].

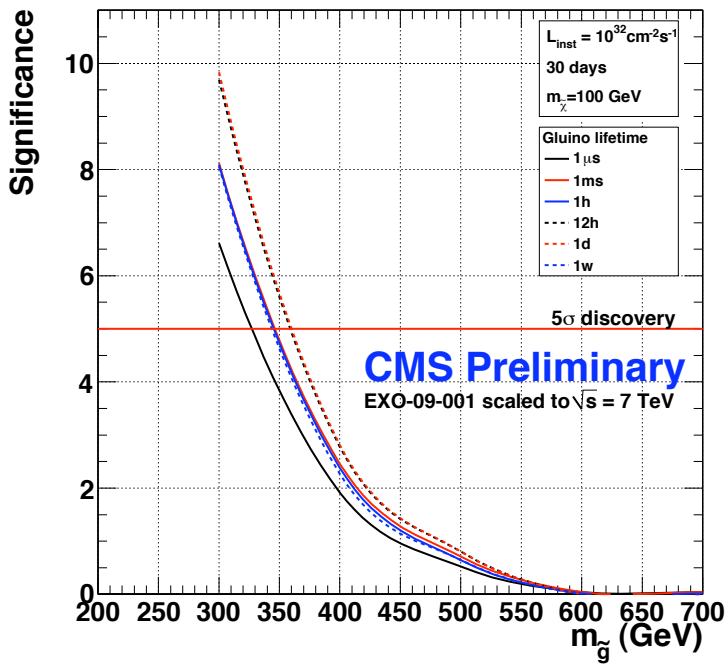


Figure 12: The discovery potential for long-lived heavy gluinos of various masses stopping in the CMS calorimeter in a 30-day long 7 TeV run at the instantaneous luminosity of $10^{32}$ cm$^{-2}$s$^{-1}$, as a function of the gluino mass and lifetime.

As a consequence, it is important to design searches that are as generic as possible. In the present discussion, we will nevertheless express the sensitivity of our searches using a scan over mSUGRA parameters, which will enable us to compare the predicted sensitivities in the early part of our program with results from the Tevatron and LEP experiments.

A second key limitation in sensitivity studies arises from our current lack of full knowledge on the backgrounds and their experimental uncertainties. As described below, the all-hadronic search involves a complex set of backgrounds, none of which is dominant. At present, it is especially difficult to reliably determine the amount of QCD background. In the like-sign dilepton search, our studies indicate that the backgrounds can be brought to a very low level. In both searches, the backgrounds and their uncertainties will largely be determined using data-driven methods. The current, Monte Carlo-based calculations for these backgrounds and their estimated systematic uncertainties are incorporated in the senstivity curves presented here. As we commission the analyses with early data, we will rapidly gain a better understanding of how large many of these backgrounds and uncertainties will be.

## 3.1 SUSY Searches in the All-Hadronic and Like-Sign Dileptons Final States

The two searches discussed here are representative of the CMS SUSY search program. Here we give a brief sketch of how these analyses are performed.

In the all-hadronic search, events with isolated muons or electrons above a certain momentum threshold (10 GeV/$c$ for muons and 15 GeV/$c$ for electrons) are vetoed, so the search is nearly independent statistically from the leptonic searches. At least three jets within a fiducial region of the detector are required above a minimal jet $p_T$ threshold ($p_T > 50$ GeV/$c$). The angle of the missing momentum vector $\mathbf{p}_T^{\rm miss}$ (which is only defined in the transverse plane) is required to point away from the leading jets, since fluctuations in the jet-energy measurement can lead to false $p_T^{\rm miss}$. Cuts on the scalar sum of transverse energies associated with the jets ($H_T$) and on the missing momentum are then imposed. For the sensitivity plots at 100 pb$^{-1}$, we have used $H_T > 400$ GeV and $p_T^{\rm miss} > 225$ GeV/$c$, whereas for 1 fb$^{-1}$, the cuts are tightened to $H_T > 500$ GeV and $p_T^{\rm miss} > 250$ GeV/$c$. Other cuts are used to help ensure the reliability of the quantities used in these selection procedures. Due to the generic nature of these requirements, the all-hadronic search typically has the highest efficiency of all our searches over mSUGRA parameter space.

Numerous standard model processes contribute to the background in the all-hadronic search. These include QCD multijet events, both with and without semileptonic decays of heavy-flavor ($b$ and $c$) quarks in jets; $Z$ + jets events with $Z \to \nu\bar{\nu}$; $W$+jets, where $W \to \ell\bar{\nu}$ (where $\ell = e$, $\mu$, and $\tau$); and $t\bar{t}$, with $t \to bW^+$ and $W^+ \to \ell^+\nu$. Several methods for data-driven background procedures are in development. The irreducible background from $Z$ + jets events with $Z \to \nu\bar{\nu}$ can be measured from $Z$ + jets events with $Z \to \mu^+\mu^-$; alternatively, a method using measurement of the $\gamma$+jets rate has shown promise in yielding a background determination with higher statistical precision [29].

The like-sign dilepton analysis has a different character: while it is less inclusive, the backgrounds are highly suppressed. The analysis is peformed in three channels: $\mu^\pm\mu^\pm$, $\mu^\pm e^\pm$, and $e^\pm e^\pm$, with the requirement of two like-sign, isolated leptons above minimum $p_T$ thresholds (both leptons with $p_T > 10$ GeV/$c$ and at least one with $p_T > 20$ GeV). A minimum of three jets above $p_T > 30$ GeV/$c$ is required, and the scalar sum of the transverse momenta of the jets must satisfy $H_T > 200$ GeV. The missing momentum in the event must satisfy $p_T^{\rm miss} > 80$ GeV/$c$.

The major contributions to the like-sign lepton background are expected to arise from $t\bar{t}$ events, where one of the leptons is produced in $W \to \ell\bar{\nu}$ decay and the other is from one of several possible sources, including $b$-hadron decay, mis-identification of a hadron, or charge-misidentification of electrons produced in $W \to e\bar{\nu}$ decay. The total estimated standard model background in a sample of 100 pb$^{-1}$ is less than 1 event.

## 3.2 Sensitivity Curves in the mSUGRA plane

The phenomenology of mSUGRA models [30] has been studied extensively in the literature, partly because these models have the attractive feature that they can be specified by just four parameters and a sign:

$$m_0, m_{1/2}, \tan\beta, A_0, \mathrm{sign}(\mu), \tag{1}$$

where $m_0$ is the common mass of the scalars at the supersymmetric GUT scale, $m_{1/2}$ is the common gaugino mass, $A_0$ is the common soft trilinear SUSY breaking parameter, $\tan\beta \equiv v_u/v_d$ is the ratio of the two Higgs vacuum expectation values, and sign($\mu$) is the sign of Higgsino mass parameter. For the CMS sensitivity scans, we have chosen $A_0 = 0$, $\tan\beta = 3$ or 10, and sign($\mu$) to be positive. With these parameters fixed, the sensitivity curves can be displayed in the plane of $m_{1/2}$ vs. $m_0$.

The sensitivity curves are based on the expected signal yield, which is a function of position in mSUGRA parameter space (due to variation in both the cross section and in the efficiency), and the expected background (and its uncertainty), which is only a function of the cuts. We have made no attempt to optimize the selection cuts as a function of position in mSUGRA space.

Figure 13 shows the 95% C.L. upper limit contours [31] for the all-hadronic search at two values of the integrated luminosity, 100 pb$^{-1}$ and 1 fb$^{-1}$, for $\tan\beta = 10$ at $\sqrt{s} = 7$ TeV. Because the physical interpretation in terms of the GUT-scale parameters $m_{1/2}$ and $m_0$ is not simple, we have included reference curves corresponding to fixed values of the gluino and squark masses. The gluino mass is roughly given by $m(\tilde{g}) \approx 2.3 m_{1/2}$. The squark masses in mSUGRA are not degenerate, with the $\tilde{t}_1$ and $\tilde{b}_1$ typically being the lightest. The squark mass used here is a representative mass from the first and second generation squarks, e.g., $u_R$, $d_R$, $s_R$, or $c_R$. As emphasized before, these mass relations and contours only have meaning within the framework of mSUGRA.

Some aspects of this plot require care in interpretation. The exclusion regions for the CDF [32] measurement are defined for $\tan\beta = 5$, while those from D0 [33] are defined for $\tan\beta = 3$. These Tevatron searches are both based on jets + missing transverse momentum signatures using approximately 2 fb$^{-1}$; we have not attempted to quantify the additional reach expected from using more data. The LEP exclusion regions are based on searches for sleptons and charginos [34]. Preliminary CMS studies of the hadronic channel indicate that its sensitivity is only weakly dependent on the value of $\tan\beta$.

Figure 14 shows the 95% C.L. upper limit contours for the like-sign dilepton search, combining the $\mu^\pm\mu^\pm$, $\mu^\pm e^\pm$, and $e^\pm e^\pm$ channels. For comparison, we show the exclusion region from recent CDF and D0 trilepton analyses [35, 36]. Both CMS and Tevatron analyses assumed $\tan\beta = 3$ in evaluating the sensitivity curves. The peaks in the sensitivity curve at low $m_{1/2}$ and for $m_{1/2} \sim 450$ GeV reflect the rate of production of like-sign dileptons in mSUGRA models.

These results indicate that in the 7 TeV run, CMS should have sensitivity to regions of SUSY (mSUGRA) parameter space beyond the current Tevatron limits. Both of the channels discussed here (all-hadronic and like-sign dileptons) should be able to yield interesting sensitivities well before 1 fb$^{-1}$.

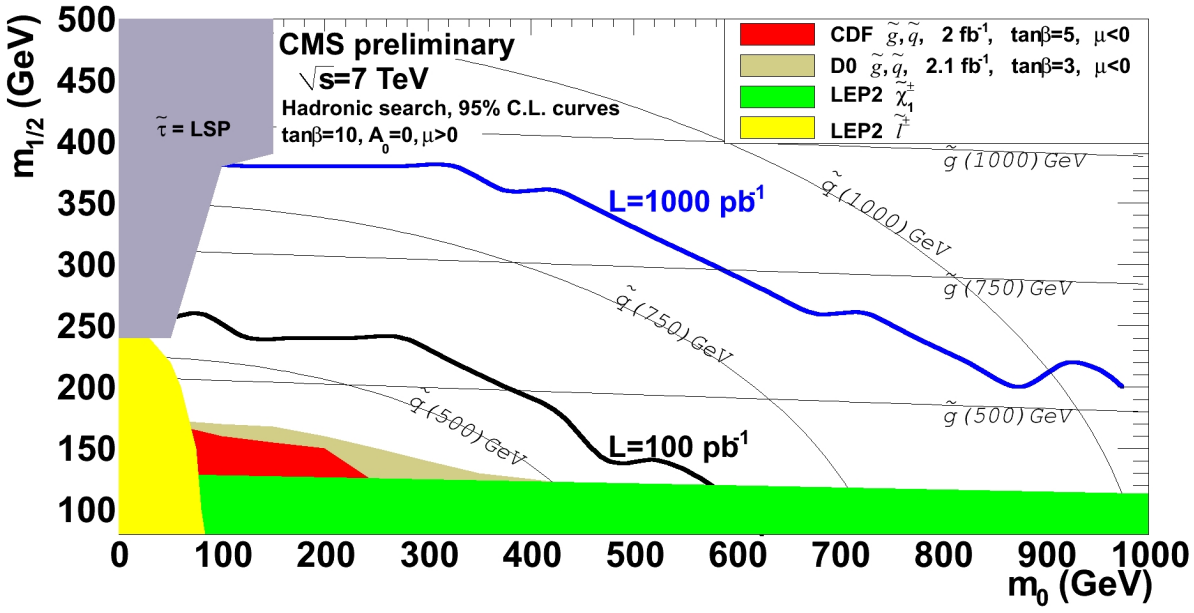


Figure 13: Estimated 95% C.L. exclusion limits for the all-hadronic SUSY search, expressed in mSUGRA parameter space.

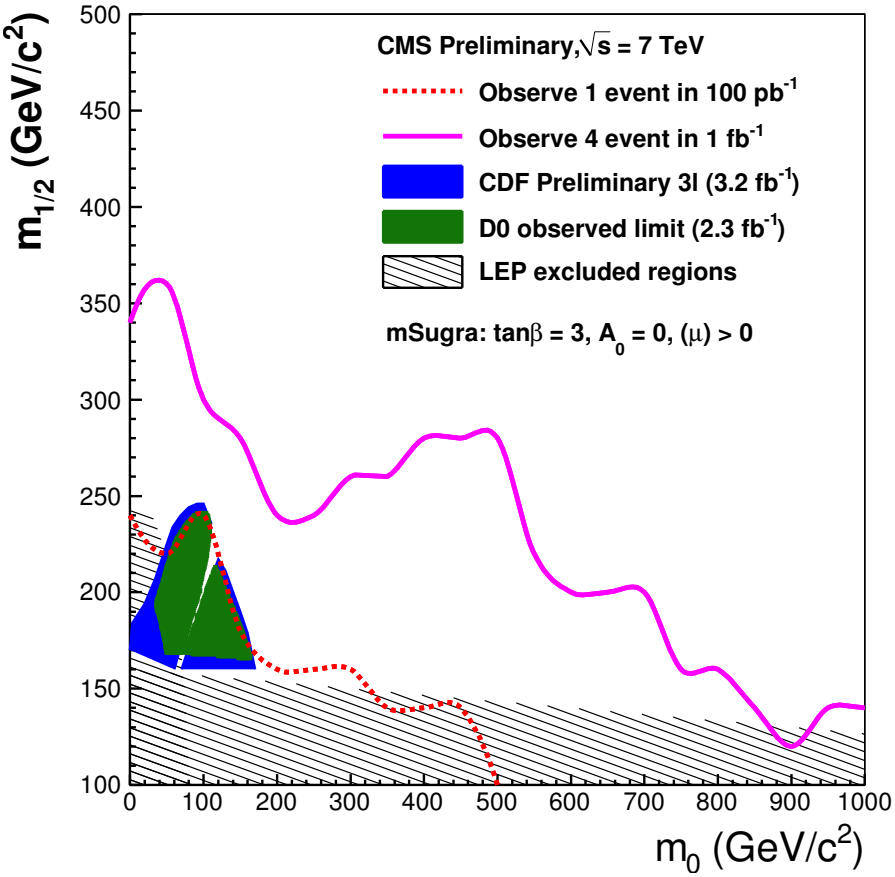


Figure 14: Estimated 95% C.L. exclusion limits for the like-sign dilepton SUSY search, expressed in mSUGRA parameter space. The expected standard model background at 100 $pb^{-1}$ (1 $fb^{-1}$) is 0.4 (4.0) events; we have assumed an observed yield of 1 event (4 events) for the purpose of setting these exclusion limits.

# 4 Higgs boson searches

The Higgs boson search sensitivity, at the center-of-mass energy of 7 TeV, for an integrated luminosity of 1 fb$^{-1}$, is discussed in this Section. The projections are based on re-scaling of the earlier published results at 14 TeV at various luminosities from 1 to 30 fb$^{-1}$. The procedure used to derive these projections is briefly outlined below.

Event yields for signal and backgrounds were re-scaled by the corresponding ratios of cross sections at 7 and 14 TeV. For the SM Higgs boson, new 7 TeV cross sections were computed as follows: gluon-gluon fusion at NNLO [37], vector-boson fusion at NLO [38], WH and ZH contributions at NLO [39], and ttH at LO [40]. For the MSSM Higgs, the $bb\Phi$ cross sections at 7 TeV and the branching ratios BR($\Phi \to \tau\tau$) were calculated using the FeynHiggs program [41]. Here, $\Phi$ stands for all three neutral Higgs bosons h, H, and A. The background event yields in the calculations used for our projections were obtained assuming NLO cross sections. For this exercise, we simply rescaled them by the ratio of 7-TeV to 14-TeV NLO cross sections, calculated using MCFM [42] and Pythia [15]. The ratios of cross sections have very little sensitivity to whether they are calculated at LO or NLO.

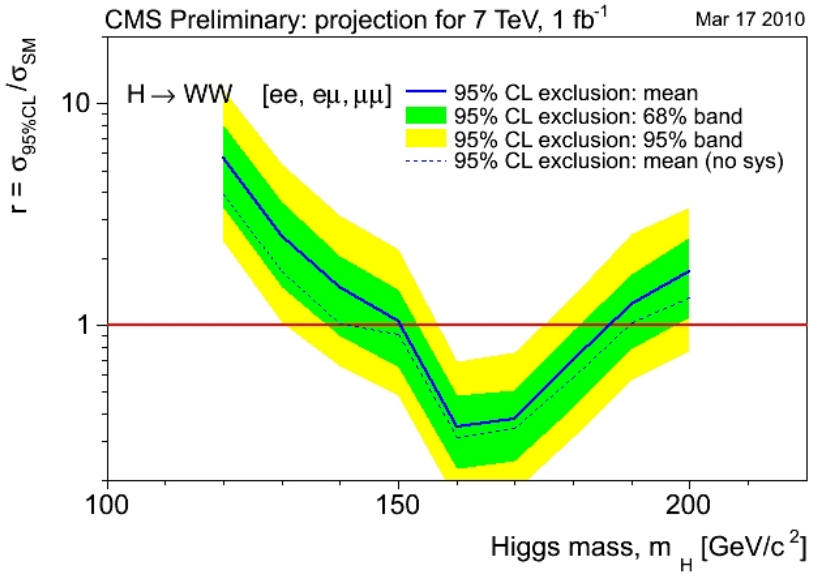


Figure 15: Expected exclusion limits for the $H \to WW \to \ell\ell\nu\nu$ search, assuming absence of signal. The expected range of exclusion is 150-185 GeV.

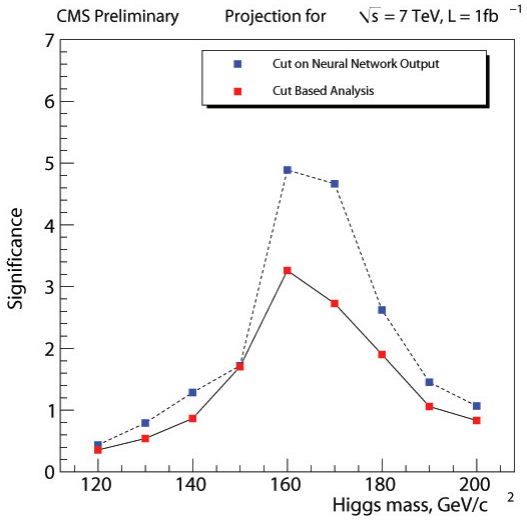


Figure 16: Expected significance for the $H \to WW \to \ell\ell\nu\nu$ search, as a function of the SM Higgs boson mass.

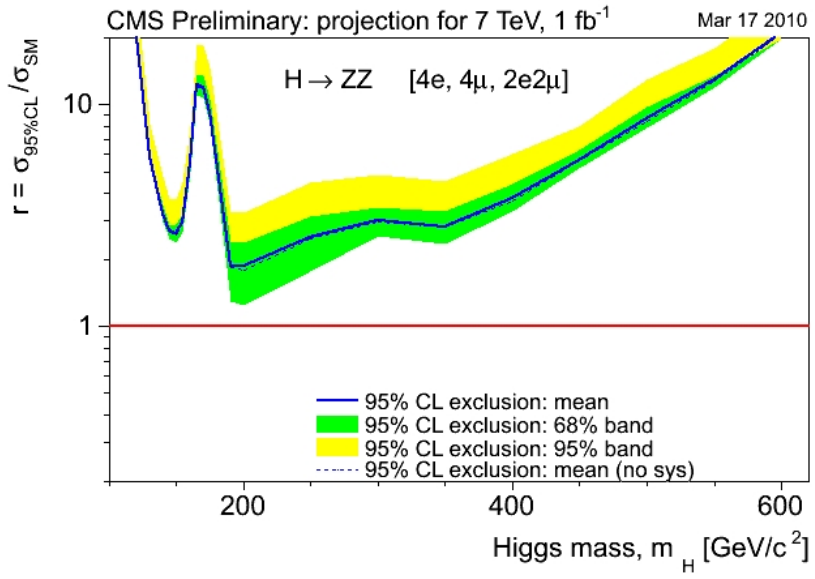


Figure 17: Expected exclusion limits for the $H \to ZZ \to 4\ell$ search, assuming absence of signal.

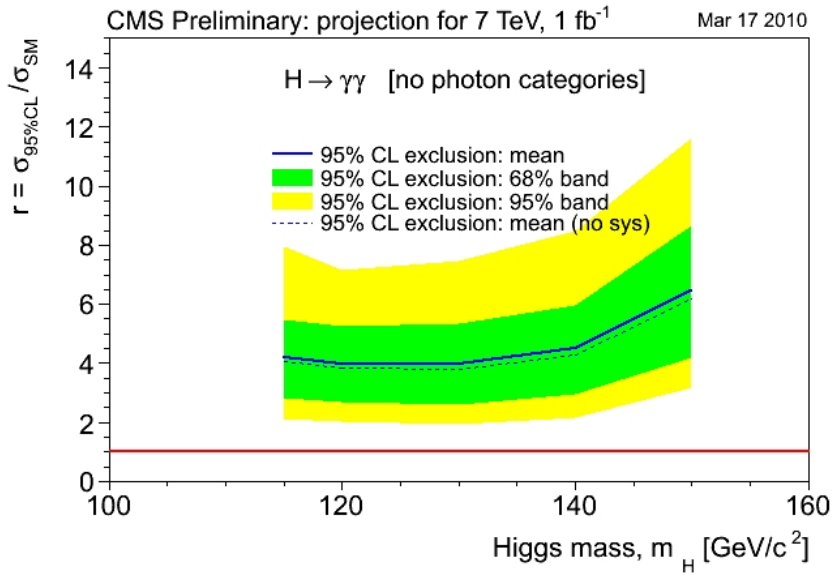


Figure 18: Expected exclusion limits for the $H \to \gamma\gamma$ search, assuming absence of signal.

While the performance of the detector reconstruction software has typically improved since the time of the previous publications, we did not include these changes into the projections presented here. Nor did we correct for a slightly higher detector acceptance at 7 TeV. (Collisions at a smaller center-of-mass energy imply that objects of a given mass are produced less boosted in the forward direction.)

Besides re-scaling event yields, the systematic errors were also extrapolated to 7 TeV and 1 fb$^{-1}$. When a particular background was derived from a control sample, we scaled the statistical error on the measured number of events in the control region, taking into account the new 7 TeV cross sections and the new target luminosity of 1 fb$^{-1}$. Remaining errors were either kept unchanged (e.g. theoretical uncertainties) or inflated to correspond to a smaller data sample.

After the event yields were re-scaled and systematic errors re-evaluated, the exclusion limits were calculated using the Modified Frequentist approach, also known as $CL_s$ [43]. The Bayesian method [44] was also exercised and, as

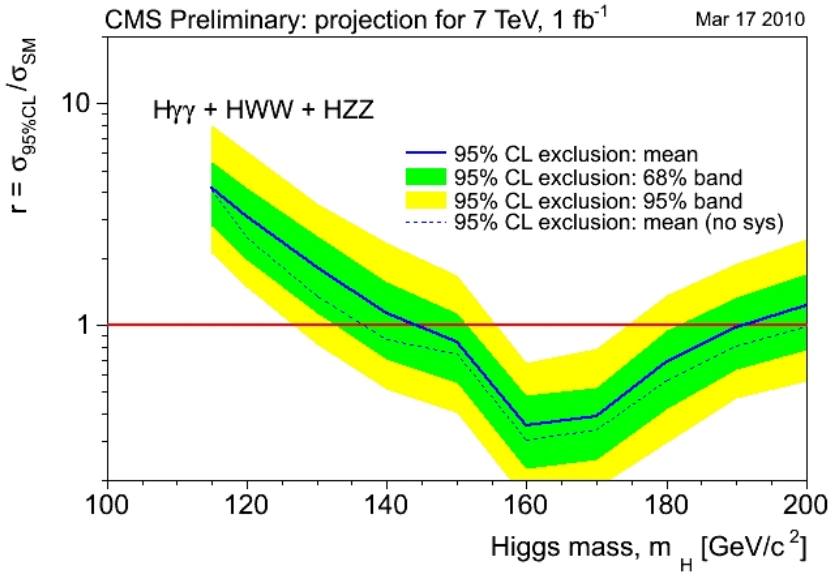


Figure 19: Expected exclusion limits for the SM Higgs, combining seven channels $H \to WW \to 2\ell 2\nu$ [$ee$, $\mu\mu$, $e\mu$], $H \to ZZ \to 4\ell$ [$4e$, $4\mu$, $2e2\mu$], and $H \to \gamma\gamma$. In absence of signal, the expected $m_H$-mass range of exclusion is 145-190 GeV.

expected, found to agree with the Modified Frequentist within 10% or better. Here, we show results obtained with the Modified Frequentist method. In the exclusion-limit plots, dashed lines show the average expected exclusion limit without systematic errors, solid lines the average with systematic errors included, and green/yellow bands indicate the expected statistical spread of the limits to be actually observed with data (68% of experimental points are expected to fall within the green bands and 95% within the yellow bands). The significance was calculated using the likelihood profile method [45].

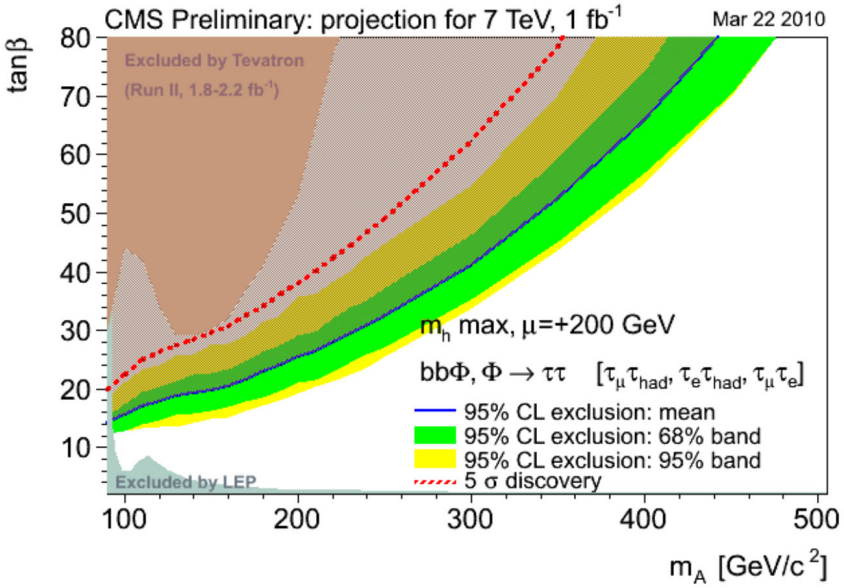


Figure 20: Expected sensitivity to the MSSM Higgs bosons in the $pp \to bb\Phi$, $\Phi \to \tau\tau$ search, with the following three final states combined: $\tau_\mu\tau_{had}$, $\tau_e\tau_{had}$, $\tau_\mu\tau_e$. The red dotted line indicates the range for a discovery-level (5-sigma) sensitivity. The solid blue line defines the range expected to be excluded at 95% C.L. in absence of signal. Regions currently excluded by LEP and Tevatron are also shown.

Figure 15 shows the projected exclusion limits for the Standard Model (SM) Higgs search in the $H \rightarrow WW \rightarrow \ell\ell\nu\nu$ decay mode. The 14-TeV analysis [46] was based on three final states $\mu\mu$, $ee$, $\mu e$ with no jets in the central part of CMS. A multivariate analysis (MVA) technique with simple event counting after cutting on the MVA output was employed. In absence of a Higgs boson, the expected range of exclusion is $150 < m_H < 185$ GeV. As seen in Fig. 16, the search using the $H \rightarrow WW \rightarrow \ell\ell\nu\nu$ channel is expected to reach a discovery level sensitivity for the SM Higgs boson in the mass range $160 < m_H < 170$ GeV.

Figure 17 shows the projected exclusion limits for the SM Higgs search in the $H \rightarrow ZZ \rightarrow 4\ell$ decay mode. Details of the original analysis can be found elsewhere [47, 48, 49, 50]. Three final states $4\mu$, $4e$, $2\mu 2e$ were included and simple event counting in optimal $4\ell$-mass windows was used. As seen in figures 15 and 17, the $H \rightarrow ZZ$ and $H \rightarrow WW$ searches have similar sensitivities for $m_H \sim 200$ GeV. Should a fourth generation of heavy quarks exists, the Higgs boson cross section in the gluon-gluon fusion would increase by a factor of 9 regardless of the fourth generation quark masses. As seen in Fig. 17, the $H \rightarrow ZZ \rightarrow 4\ell$ search should be enough for excluding an Higgs boson with a mass up to about 500 GeV, in the four-generation scenario.

Figure 18 shows the projected exclusion limits for the $H \rightarrow \gamma\gamma$ search. Details of the original analysis can be found elsewhere [51]. For the purposes of this projection, we used a conservative option of not distinguishing between reconstructed photon categories and simply counting events in an optimal $\gamma\gamma$-mass window. As it is well known, the $H \rightarrow \gamma\gamma$ search is expected to have the best sensitivity to the SM Higgs boson at the low mass range. The projection presented here is for a generic search for a narrow $\gamma\gamma$ resonance, since nothing specific to the SM Higgs boson was utilized in this study.

Figure 19 shows the projected exclusion limits for a combination of the seven channels presented above, namely: three $H \rightarrow WW$ channels, three $H \rightarrow ZZ$ channels, and one $H \rightarrow \gamma\gamma$ channel. All these channels are important to achieve the best coverage for the full range of possible SM Higgs boson masses. When combined together, the expected exclusion limit for the SM Higgs at 7 TeV and with 1 fb$^{-1}$ becomes $145 < m_H < 190$ GeV.

Figure 20 shows the projected sensitivity for the MSSM Higgs bosons in the $pp \rightarrow bb\Phi$, $\Phi \rightarrow \tau\tau$ search. The following three final states were used: $\tau_\mu\tau_{had}$ [52], $\tau_e\tau_{had}$ [53], $\tau_\mu\tau_e$ [54], where $\tau_\mu$ stands for the $\tau \rightarrow \mu\nu\nu$ decay, $\tau_e$ stands for the $\tau \rightarrow e\nu\nu$ decay, and $\tau_{had}$ stands for the hadronic $\tau$-decays with one or three charged pions. The analysis strategy is based on the use of b-tagging, reconstructing the final $\tau\tau$ final states, and counting events in optimal $m_{\tau\tau}$ mass windows. Figure 20 shows the expected sensitivity of such a search interpreted in the context of the MSSM $m_h^{max}$-scenario [55]. At 7 TeV and with a 1-fb$^{-1}$ data sample, we can expect to reach a discovery level sensitivity in a large not-yet-explored range of the $(m_A, tan\beta)$-plane, covering $tan\beta > 20$ at low $m_A$. In the absence of signal, the exclusion range drops down even deeper to values of $tan\beta \sim 15$ at low $m_A$.

# References


[1] CMS Collaboration, *CMS Technical Design Report, Vol. II: Physics Performance*, J. Phys. G **34**, 995 (2007) .

[2] http://cdsweb.cern.ch/collection/CMS Physics Analysis Summaries?ln=en

[3] CMS Collaboration, CMS PAS EXO-09-012 (2009).

[4] CMS Collaboration, CMS PAS EXO-09-004 (2009).

[5] CMS Collaboration, CMS PAS EXO-09-009 (2009).

[6] CMS Collaboration, CMS PAS EXO-09-013 (2009).

[7] CMS Collaboration, CMS PAS EXO-09-004 (2009).

[8] CMS Collaboration, CMS PAS EXO-08-010 (2008).

[9] CMS Collaboration, CMS PAS EXO-09-010 (2009).

[10] CMS Collaboration, CMS PAS SBM-07-002 (2007).

[11] CMS Collaboration, CMS PAS EXO-08-003 (2008).

[12] CMS Collaboration, CMS PAS EXO-09-001 (2009).

[13] J. Stirling, private communication.

[14] A.D. Martin, W.J. Stirling, R.S. Thorne, and G. Watt, Eur. Phys. J. **C63**, 189 (2009); *ibid.* **C64**, 653 (2009).

[15] **Pythia**: T. Sjstrand, S. Ask, R. Corke, S. Mrenna, P. Skands, http://home.thep.lu.se/ torbjorn/Pythia.html

[16] T. Aaltonen *et al.* (CDF Collaboration), e-print arXiv:0912.1057, submitted to PRL.

[17] V.M. Abazov *et al.* (DØ Collaboration), Phys. Rev. Lett. **102**, 051601 (2009); *ibid.*, **103**, 191803 (2009).

[18] T. Aaltonen *et al.* (CDF Collaboration), Phys. Rev. Lett. **99**, 171801 (2007); V.M. Abazov *et al.* (DØ Collaboration), Phys. Rev. Lett. **100**, 091802 (2008).

[19] T. Aaltonen *et al.* (CDF Collaboration), Phys. Rev. Lett. **102**, 091805 (2009); *ibid.* **102**, 031801 (2009)

[20] V.M. Abazov *et al.* (DØ Collaboration), Phys. Rev. Lett. **101**, 011601 (2008); T. Aaltonen *et al.* (CDF Collaboration), Phys. Rev. Lett. **101**, 181602 (2008).

[21] D. Acosta *et al.* (CDF Collaboration), Phys. Rev. D Brief Reports **72**, 051107 (2005); A. Abulencia *et al.* (CDF Collaboration), Phys. Rev. D Brief Reports **73**, 051102 (2006); V.M. Abazov *et al.* (DØ Collaboration), Phys. Lett. B **671**, 224 (2009); *ibid.* **681**, 224 (2009).

[22] V.M. Abazov *et al.* (DØ Collaboration), DØ Note 4577-CONF, `http://www-d0.fnal.gov/Run2Physics/WWW/results/prelim/NP/N20/N20.pdf` (2004); DØ Note 5923-CONF, `http://www-d0.fnal.gov/Run2Physics/WWW/results/prelim/NP/N66/N66.pdf` (2009).

[23] V.M. Abazov *et al.* (DØ Collaboration), Phys. Rev. Lett. **102**, 161802 (2009); T. Aaltonen *et al.* (CDF Collaboration), Phys. Rev. Lett. **103**, 021802 (2009).

[24] V.M. Abazov *et al.* (DØ Collaboration), Phys. Rev. Lett. **99**, 131801 (2007).

[25] S. Martin, arXiv:hep-ph/9709356v5; H. Baer and X. Tata, *Weak Scale Supersymmetry*, Cambridge University Press, Cambridge (2006); M. Drees, R. Godbole, and P. Roy, *Theory and Phenomenology of Sparticles*, World Scientific, Singapore (2005).

[26] C. Berger, J. Gainer, J. Hewett, and T. Rizzo, JHEP 0902:023 (2009); arXiv:0812.0980v3.

[27] N. Arkani-Hamed *et al.*, arXiv:hep-ph/0703088.

[28] J.Alwall, P. Schuster, and N. Toro, Phys. Rev. D **79**, 075020 (2009); arXiv:0810.3921.

[29] CMS Collaboration, CMS PAS SUSY-08-002 (2008).

[30] A. Chamseddine. R. Arnowitt, and P. Nath, Phys. Rev. Lett. **49**, 970 (1982); E. Cremmer, P. Fayet, and L. Girardello, Phys. Lett. B **122**, 41 (1983); see also S. Martin, arXiv:hep-ph/9709356v5, p. 78.

[31] J. Conway, *Calculation of Cross Section Upper Limits Combining Channels Incorporating Correlated and Uncorrelated Systematic Uncertainties*, CDF/Pub/Statistics/Public/6428 (2005).

[32] CDF Collaboration (T. Altonen *et al.*, Phys. Rev. Lett. **102**, 121801 (2009); arXiv.org:0811.2512; the CDF exclusion region in the $m_{1/2}$ vs. $m_0$ plane appears in CDF Public Note 9229, March 2008.

[33] D0 Collaboration (V.M. Abazov *et al.*), Phys. Lett. B **660**, 449 (2008); arXiv.org:0712.3805.

[34] LEPSUSYWG; ALEPH, DELPHI, L3, and OPAL Collaborations, note LEPSUSYWG/02-06.2, http://lepsusy.web.cern.ch/lepsusy.

[35] CDF Collaboration, *Update of the Unified Trilepton Search with 3.2 $fb^{-1}$ of Data*, CDF/PUB/EXOTIC/PUBLIC/9817 (2009).

[36] D0 Collaboration, V. Abazov *et al.*, Phys. Lett. B **680**, 34 (2009).

[37] **HggTotal**: C. Anastasiou, R. Bougezhal, F. Petriello, JHEP 0904:003 (2009).

[38] **VV2H**: M. Spira, http://people.web.psi.ch/spira/vv2h/

[39] **V2HV**: M. Spira, http://people.web.psi.ch/spira/v2hv/

[40] **HQQ**: M. Spira, http://people.web.psi.ch/spira/hqq/

[41] G. Degrassi, M. Frank, T. Hahn, S. Heinemeyer, W. Hollik, H. Rzehak, P. Slavich, G. Weiglein *FeynHiggs program for calculating MSSM Higgs properties*, http://www.feynhiggs.de/; also, hep-ph/0611326, hep-ph/0212020, hep-ph/9812472, hep-ph/9812320.

[42] **MCFM**: J. M. Campbell and R. K. Ellis, http://mcfm.fnal.gov/

[43] A. L. Read, *Modified frequentist analysis of search results (the $CL_s$ method)*, CERN-OPEN-2000-205; also, J. Phys. G **28**, 2693 (2002).

[44] e.g., A. OHagan, *Kendalls Advanced Theory of Statistics, Volume 2B: Bayesian Inference* (Edward Arnold, London, 1994); H. Jeffreys, *Theory of Probability* (Oxford University Press, Oxford, 1961), 3rd ed.

[45] e.g., Thomas Alan Severini, *Likelihood methods in statistics* (Oxford University Press, 2000).

[46] CMS Collaboration, *Search Strategy for a Standard Model Higgs Boson Decaying to Two W Bosons in the Fully Leptonic Final State*, CMS PAS HIG-2008/006.

[47] CMS Collaboration, *Search strategy for the Higgs boson in the $ZZ^{(*)}$ decay channel with the CMS experiment*, CMS PAS HIG-2008/003.

[48] S. Baffioni et al., *Discovery potential for the SM Higgs boson in the $H \to ZZ^{(*)} \to e^+e^-e^+e^-$ decay channel*, CMS NOTE 2006/115.

[49] S. Abdullin et al., *Search Strategy for the Standard Model Higgs Boson in the $H \to ZZ^{(*)} \to \mu^+\mu^-\mu^+\mu^-$ Decay Channel using $m_{4\mu}$-Dependent Cuts*, CMS NOTE 2006/122.

[50] D. Futyan et al., *Search for the Standard Model Higgs Boson in the Two-Electron and Two-Muon Final State with CMS*, CMS NOTE 2006/136.

[51] M. Pieri et al., *Inclusive Search for the Higgs Boson in the $H \to \gamma\gamma$ Channel*, CMS NOTE 2006/112.

[52] A. Kalinowski et al, *Search for MSSM heavy neutral Higgs boson in $\tau + \tau \to \mu + jet$ decay mode*, CMS NOTE-2006/105.

[53] R. Kinnunen and S. Lehti, *Search for the heavy neutral MSSM Higgs bosons with the H/A $\to \tau\tau \to$ electron + jet decay mode*, CMS NOTE 2006/075.

[54] S. Lehti, *Study of MSSM $H/A \to \tau\tau \to e\mu + X$ in CMS*, CMS NOTE 2006/101.

[55] M. Carena, S. Heinemeyer, C.E.M. Wagner and G. Weiglein, *Suggestions for Benchmark Scenarios for MSSM Higgs Boson Searches at Hadron Colliders*, hep-ph/0202167.